Optimization Of The Low-High-Low Structure In GaN (Wz) SDR Impatt Diode For Enhanced Millimeter Wave Performance

B. Chakrabarti, D. Ghosh, L.P. Mishra, M. Mitra

Abstract: Extensive simulation experiments have been done on GaN (Wz) based single-low-high-low (SLHL) IMPATT Devices at W-band to study the d.c. and small signal characteristics. In this paper it is well established that the height (doping density of the bump), width, and position of the charge bump are the major decisive parameters in improving the performance of the diode. It has been observed that by varying height and width of the bump the performance of IMPATT can be enhanced. Diode efficiency of 20.23% and power output of 1.21W are achieved by changing the position of the bump. Different values of width of the bump do not affect that much into the performance the diode. The analysis here is extremely useful for further improvement of SLHL structure of IMPATT to achieve better overall response.

Index Terms: GaN IMPATT, Charge bump, W-band IMPATT, small signal response, RF power, negative resistivity

1 INTRODUCTION

IMPATT diodes have emerged as the most powerful solid state sources of microwaves, millimeter waves and sub-millimeter waves covering a wide range of frequency spectrum. The vast frequency range of operation and high power output have made the IMPATT diodes as highly suitable devices to meet the ever increasing communication needs of the world. Extensive research is being carried out to produce high power solid state millimeter and sub-millimeter wave sources with effectively high efficiency which can operate at high temperature. High breakdown voltage is required for the generation of high power and high thermal conductivity is required for good thermal stability of the device. The wide band gap semiconductors such as SiC and GaN having high critical electric field and high thermal conductivity are suitable materials for this purpose. A recent review work on wide band gap semiconductor establishes the superiority of GaN based high power and high frequency devices [1].

The RF power output from IMPATT diode may be increased by increasing the operating current density. At this high value of current density the mobile space charge effect become dominant which reduces the device efficiency and negative conductivity and therefore the overall performance of the device degrades. It has been observed that with the modified low-high-low (known as SLHL) doping profile of the depletion region [2] the effect of the mobile space charge can be reduced and the diode performance in terms of negative conductance, efficiency and power output can be improved. Experimental investigations were carried out for Si based flat and low-high-low type DDR IMPATT diodes at V band [3]. Luy et. al. also reported [4] the fabrication of Si low-high-low DDR diodes using MBE technique. The test result shows a maximum efficiency of 17.6% and continuous power of 800mw at 67 GHz. Experimental results are also reported for Si based low-high-low diodes fabricated at D-band with 300mw of RF power at around 140GHz with efficiency 8% [5]. All these previous experimental studies have revealed the advantages of low-high-low structure over its flat profile Si counterpart. Studies also reported on DDR IMPATT diodes for 4H-SiC material by Mukerjee et. al. [6] at Ka and D band respectively and established the superiority of L-H-L type devices over flat devices. The parameters of the impurity charge bump that is **(i)** doping density of the bump **(ii)** the width of the bump **(iii)** the position of the bump with respect to the metallurgical

- B.Chakrabarti is currently working as asst. prof. in the Dept. of Electronics & Communication Engineering, Bengal Institute of Technology, Kolkata150, India. E-mail: chakrabortybibek@yahoo.co.in
- D. Ghosh is currently working as asst. prof. in the Dept. of Electronics & Communication Engineering, Swami Vivekananda Institute of Science and Technology, Kolkata-145, India. E-mail: dg1036@yahoo.com
- L.P. Mishra is currently working as asst. prof. in the Dept. of Electronics & Communication Engineering, ITER, SOA University,Bhubaneswar, India. E-mail: lp_mishra@yahoo.co.in
- M. Mitra is currently working as associate prof. in the Dept. of Electronics & telecommunication, BESU, Shibpur, Howrah 711103,W.B., India. E.mail:- monojit_m1@yahoo.co.in.

junction play important role in determining the d.c and small signal performance of the diode. In this paper, authors have thoroughly studied the effect of the variation of the parameters of the charge bump on the d.c and small signal performance at W-band for GaN (Wz) SDR IMPATT diode. The elaborated studies are made on the electric field profiles, normalized current density profiles, RF power output, admittance characteristics and also on device total negative resistivity. To the best of our knowledge this is the first comparative study on the mm wave characteristics of GaN (Wz) based SDR (SLHL) IMPATT diodes at W-band frequency.

2 COMPUTER SIMULATION TECHNIQUE

In this paper SDR IMPATT (GaN based) with low-high-low (SLHL) doping profile of the depletion region has been studied. The device dimension, doping and current densities are considered for W-band operation. The impurity bump (charge spikes) is incorporated into the flatly doped of SDR (p^{++} n n^{++}) on the n-side of the metallurgical junction in such a way that a lightly doped region is located between the junction and the impurity bump to give rise to a single low-high-low (SLHL) SDR structure (p^{++} n n^{+} n n^{++}). Typical schematic diagram and doping profile of the SLHL SDR IMPATT diode considered in the simulation experiment is shown in figure 1. The origin (x=0) of the coordinate system is taken at the metallurgical junction. The doping concentration at the metallurgical junction and at the interface of epitaxy and substrate ($x>|W_n|$) is described by appropriate exponential and complementary error function profile. The depletion layer width is equal to W_n. The doping concentration at different regions of the diode can be written as

$N(x) = N_1[1-\exp(x/s)]$ for the region $0>x>-W_1$ where s is the curvature of the doping profile

$N(x) = N_2$ for the region, $-W_1> x >-W_2$

$N(x) = N_1$ for the region, $-W_2> x >-W_n$

Also, $N(x) = N_h\exp(-1.08\lambda-0.78\lambda^2)$ for n^{++} n interface of epitaxy and substrate.

Where $\lambda = x/2(Dt)^{1/2}$, for which D is the diffusion constant for impurity atoms, x is the distance from the surface and t is the time of diffusion. The value for $(Dt)^{1/2}$ has been taken 4μm. Substrate doping is taken a very high value ($5\times10^{26}m^{-3}$) for the present analysis. The values N_1 and N_2 are the doping concentrations for the lightly and highly doped (bump) regions respectively. The constant "λ" involved in the expression is taken as 5 nm.

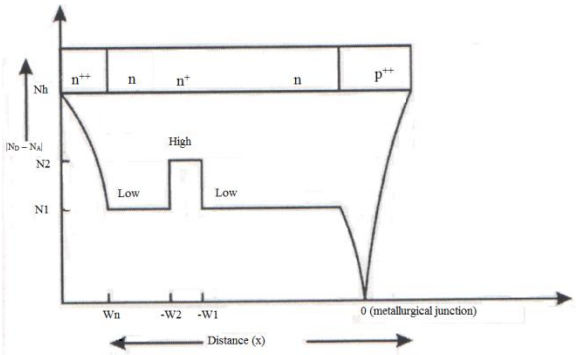

Figure 1. Schematic structure and doping profile for single drift SLHL IMPATT diode: N_1 = low epilayer doping concentration, N_2 = high epilayer doping concentration, N_h = substrate doping concentration, W_1 - W_2 = bump width, Wn= total width of the epilayer.

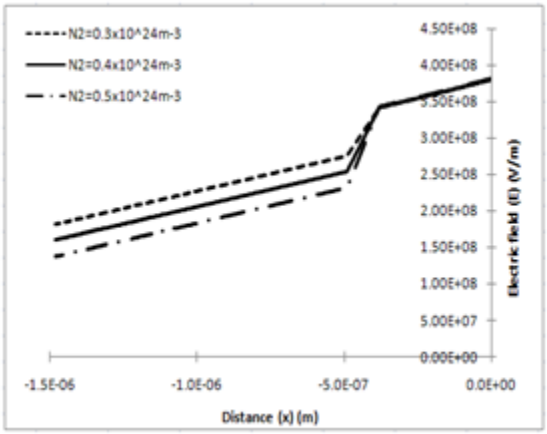

Figure 2. Distance vs electric field of GaN SDR SLHL IMPATT diode for different values of doping density of the charge bump at W-band.

The bump width can be calculated as $\delta_n = |W_2 - W_1|$ on the n-side and the depletion width for W-band operation is chosen from the transit time formula $W_n = 0.37V_n/f_0$.. Where V_n is the saturation drift velocity of electrons and f_o is the design frequency. The junction temperature is taken constant at 300K. For the present simulation work experimental values of carrier ionization rates, temperature dependent (300k<T<600k) values of drift velocity and mobility of charge carriers in GaN (Wz) are considered [7, 8, 9] .

2.1 D.C Analysis

The DC analysis has been carried out and optimized through a double iterative simulation technique of IMPATT action explained elsewhere [10].The simulation process is initiated by suitable choice of the edges of the active zone by solving the Poisson's equation

$$dE/dx = q/\varepsilon(N_D - N_A + p(x) - n(x)) \quad (1)$$

Where N_D is the ionized donor density and N_A is the ionized acceptor density, n and p are electron and hole densities respectively. The fundamental device equations are numerically solved by the generalized double iterative simulation algorithm to obtain electric field and normalized current density profiles. Avalanche breakdown occurs around the junction where the electric field is large enough such that charge multiplication factors (M_n,M_p) become infinite. The breakdown voltage can be calculated by integrating the field profile over the entire depletion layer width; i.e.

$$V_B = \int_0^{Wn} E(x)dx \quad (2)$$

where W_n represents depletion layer width. The device efficiency is calculated from the approximate formula

$$\eta\ \% = (V_D)*(100/\pi)/V_B \quad (3)$$

where V_D is the voltage drop across the drift region. Also $V_D = V_B - V_A$, where V_A is the voltage drop across the avalanche region.

2.2 Small signal Analysis

The range of frequencies exhibiting negative conductance of the diode can easily be computed by Gummel-Blue method [11]. The dc electric field and current density profiles, which are obtained from the D.C analysis, are fed as input data for the small signal analysis. The real part R(x, ω) and imaginary part X(x, ω) are obtained by splitting the diode impedance Z(x, ω) using Gummel-Blue method and thus two different equations are framed [12]. Then, by using modified Runga-Kutta method [13] the solutions of these two equations are found following a double iterative simulation scheme.

The small signal parameters like negative conductance(-G), susceptance (B), impedance (Z) of the diode and the range of frequencies over which the diode exhibits negative conductance are found after satisfying the boundary conditions derived elsewhere [14,15].

The diode negative resistance ($-Z_R$) and reactance ($-Z_x$) at a particular frequency (ω) can be determined from numerical integration of the resistivity (-R(x)) and reactivity (–X(x)) profiles over the depletion layer.

Thus

$$-Z_R = \int_0^{Wn} -R\ dx \quad \text{and}$$
$$-Z_X = \int_0^{Wn} -X dx \quad (4)$$

The diode total impedance Z is obtained by,

$$Z_{total} = \int_0^{Wn} Z(x,\omega)dx = -Z_R + jZ_x \quad (5)$$

The diode admittance is expressed as

$Y = 1/Z = -G + jB = 1/(-Z_R + jZ_x)$ and diode total negative conductance and susceptance have been calculated from the following formulas

$$\text{or,} \quad G = -Z_R/((Z_R)^2 + (Z_x)^2) \quad \text{and}$$
$$B = Z_x/((Z_R)^2 + (Z_x)^2) \quad (6)$$

G and B are both normalized to the diode area.

The Avalanche (resonance) frequency (f_a) is a frequency at which the imaginary part, susceptance (B) of the admittance changes its nature from inductive to capacitive. The small signal quality factor (Q_P) is defined as the ratio of the imaginary part of the admittance (B) to the conductance (G)(at the peak frequency), i.e.

$$-Q_P = (B_P/-G_P) \quad (7)$$

At a given bias current density, the peak frequency (f_P) is the frequency at which the magnitude of the negative conductance of diode is the maximum. At f_P, the maximum RF power (P_{RF}) from the device is obtained from the expression.

$$P_{RF} = (V^2_{RF}).|-G_P|.A/2 \quad (8)$$

The area of the diode is considered to be $5x10^{-11}$ m^2. Under small signal condition V_{RF} (the amplitude of the RF swing) is taken as $V_B/5$.

3 RESULTS AND DISCUSSION

The optimized design parameters for GaN (Wz) SDR IMPATT (SLHL) diodes at W frequency bands are shown in table1a, 1b & 1c respectively. The effects on the D.C and Small Signal properties due to the variations of the various parameters of the impurity bump such as i) doping density of the bump ii) width of the bump and iii) position of the bump with respect to the metallurgical junction, are summarized in table 1a, 1b, 1c & table 2a, 2b, 2c respectively.

TABLE 1a

DC analysis of GaN (wz) IMPATT diode due to variation of the doping density(N_2) of the impurity charge bump where $N_1=0.5\times10^{23}m^{-3}$, $J_{dc}=1.5\times10^{8}A/m^{-2}$ and $W_n=1.48\times10^{-6}m$, $W_1=0.38$ μm, δn = 0.11μm

N_2 ($10^{24}m^{-3}$)	V_A (V)	V_B (V)	η (%)
0.3	173	396	17.9
0.4	148	375	19.2
0.5	144	353	18.4

TABLE 1b

DC analysis of GaN (wz) IMPATT diode due to variation of the width(δn) of the impurity charge bump, where $N_1=0.5\times10^{23}m^{-3}$, $J_{dc}=1.5\times10^{8}A/m^{-2}$ and $W_n=1.48\times10^{-6}m$, $W_1=0.38$ μm, $N_2=0.4\times10^{24}m^{-3}$

δn (μm)	V_A (V)	V_B (V)	η (%)
0.09	157	388	18.9
0.11	148	375	19.2
0.13	147	361	18.8

TABLE 1c

DC analysis of GaN (wz) IMPATT diode due to variation of the position(W_1) of the impurity charge bump, where $N_1=0.5\times10^{23}m^{-3}$, $J_{dc}=1.5\times10^{8}A/m^{-2}$ and $W_n=1.48\times10^{-6}m$, δn = 0.11μm, $N_2=0.4\times10^{24}m^{-3}$

W_1 (μm)	V_A (V)	V_B (V)	η (%)
0.32	136.5	375	20.2
0.38	148	375	19.2
0.42	159	375	18.3

The d.c simulation program as described earlier is used to obtain the E(x) and P(x) profiles. The electric field profile (E(x)) of the SLHL type GaN (Wz) SDR IMPATT diodes for different doping density of the bump are shown in fig 2. It can be observed from the figure that the value of the maximum electric field at the junction does not change appreciably for changing the doping density of the impurity bump. As the doping density of the impurity bump is increasing the electric field decreasing at a faster rate (fig. 2) in the bump region and therefore the overall area under the electric field profile is decreasing. It in turn signifies that the space charge effect is largely reduced due to high doping density of the bump and hence localization of the Avalanche region and reduction of the value of Avalanche voltage (V_A) is obtained (table 1a,1b & 1c). An efficiency of 20.2% can be obtained with the value of W_1= 0.32μm.The breakdown voltage (V_B) is also seen to decrease with the increment of the doping density of the bump. The same decreasing trend of V_A and V_B can be observed for increasing the bump width (δn). However as the distance of the bump from metallurgical junction is increasing the opposite trend of V_A that is decrement of V_A is seen though break down voltage (V_B) value remains at constant value. Therefore as the position of bump shifts nearer to the metallurgical junction, the efficiency of the diode increases (table 1c). The admittance characteristics and negative resistivity profiles within the depletion layer of IMPATT for different parameters of the impurity bump are obtained from small signal simulation program as explained earlier. The integrated mm-wave properties of the device such as negative conductance, susceptance, RF power, quality factors can be obtained from admittance characteristics of the diodes. The variation of the conductance and suceptance with frequencies at W-band for GaN (Wz) SDR IMPATT diodes for different input impurity bump parameters are shown in figure 3a, 4a & 5a respectively. It can also be observed from table-2a & 2b that the magnitude of peak negative conductance ($-G_P$) at the peak frequency increases as the doping density of the bump and also the width of the bump increases.

Considering the output RF power (P_{RF}), its value decreases as the doping density of the bump and the distance of the bump from metallurgical junction increases, but it does not change considerably if the width of the bump is varied. Better value of the quality factors (Q_P) can be obtained with the increasing of doping density of the bump and decreasing of the distance of the impurity bump from

metallurgical junction. The spatial distribution of the negative resistivity profile R(x) at the peak frequency (f_P) in the depletion layer gives us clear insight into the contribution to the RF power by the depletion layer. The computed R(x) profiles shows a negative maxima in the middle(approximately) of the drift region (n-region) and negative minima near the metallurgical junction(Figure 3b,4b,5b).From the figure 3b and 5b it can be observed that as the doping density of the impurity bump increases and the distance of the bump from metallurgical junction decreases the magnitude of the negative resistivity maxima (peak) as well as the negative resistivity minima increases where as changing of the width of the bump does not does not affect appreciably. Thus the diode total negative resistance ($-Z_{RP}$) at the peak frequency increases as the doping density of the bump increases and the bump comes

TABLE 2a

Small signal results of GaN (wz) IMPATT diode due to variation of the doping density(N_2) of the impurity charge bump, where W_1 = 0.38μm, δn = 0.11μm

N_2 ($10^{24}m^{-3}$)	f_P (GHz)	$-G_P$ (10^7 Sm^{-2})	P_{output} (W)	Q_P	$-Z_{RP}$ (10^{-7} Ωm^2)
0.3	89.5	0.726	1.13	3.12	0.127
0.4	90	0.760	1.06	2.97	0.133
0.5	85	0.818	1.01	2.39	0.179

TABLE 2b

Small signal results of GaN (wz) IMPATT diode due to variation of the width(δn) of the impurity charge bump, where W_1=0.38 μm, N_2=0.4x$10^{24}m^{-3}$

(δn) (μm)	f_P (GHz)	$-G_P$ (10^7 Sm^{-2})	P_{output} (W)	Q_P	$-Z_{RP}$ (10^{-7} Ωm^2)
0.09	90	0.708	1.06	3.19	0.125
0.11	90	0.760	1.06	2.97	0.133
0.13	92	0.788	1.03	3.00	0.125

TABLE 2c

Small signal results of GaN (wz) IMPATT diode due to variation of the position(W_1) of the impurity charge bump, where δn = 0.11μm, N_2=0.4x$10^{24}m^{-3}$

W_1 (μm)	f_P (GHz)	$-G_P$ (10^7 Sm^{-2})	P_{output} (W)	Q_P	$-Z_{RP}$ (10^{-7} Ωm^2)
0.32	87	0.861	1.21	2.33	0.179
0.38	90	0.760	1.06	2.97	0.133
0.42	89	0.628	0.8	3.5	0.118

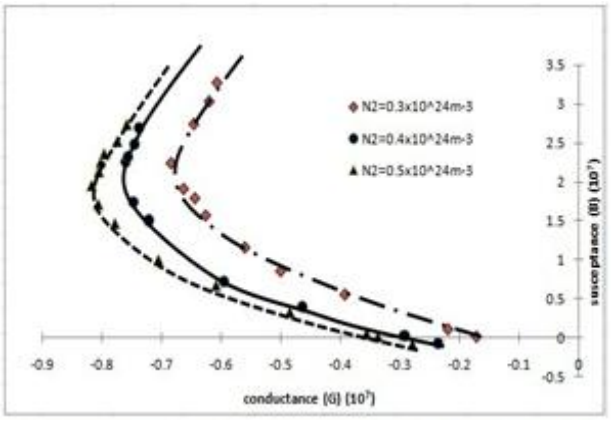

Figure 3(a). Conductance (G) vs susceptance (B) plot for different values of doping density of the charge bump.

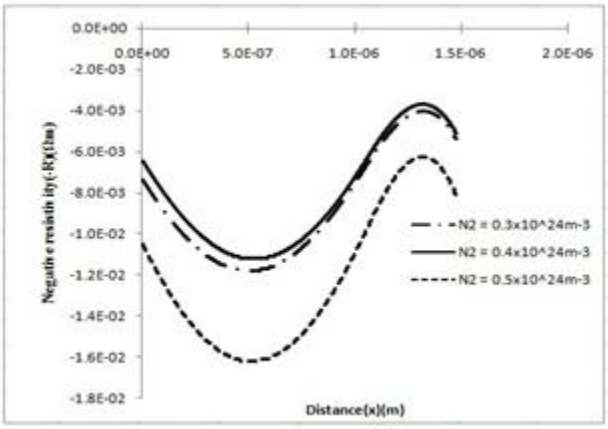

Figure 3(b). Negative resistivity profile for different values doping density of the charge bump.

closer to the junction whereas it does not show appreciable change due to the variation of the width of the bump (table-2a & 2c). Figure (5b) also suggests that the position of the negative resistivity peak slightly shifts away from the junction as the distance of the bump from the metallurgical junction increases. The present d.c and small signal analysis thus gives useful and interesting results regarding the role of various parameters of the impurity charge bump in improving the performance of GaN(Wz) SDR diodes.

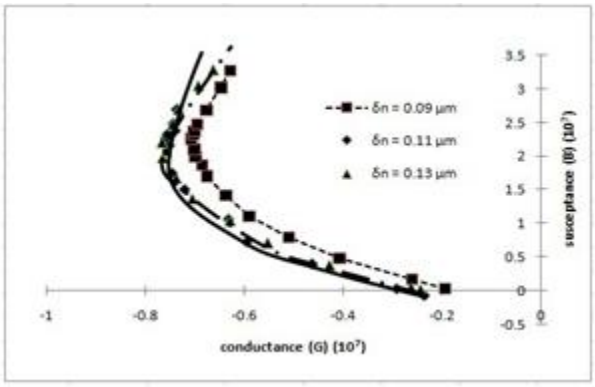

Figure 4(a). Conductance (G) vs susceptance (B) plot for different values of width (δn) of the charge bump.

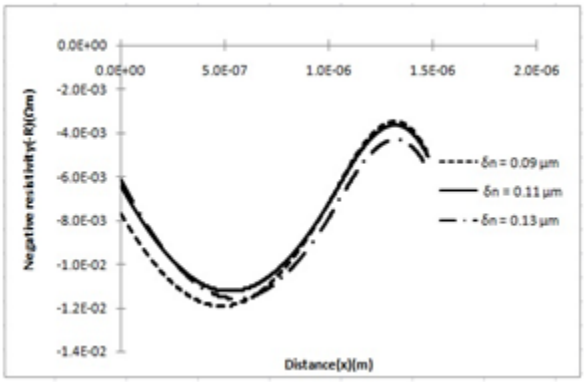

Figure 4(b). Negative resistivity profile for different values of width (δn) of the charge bump.

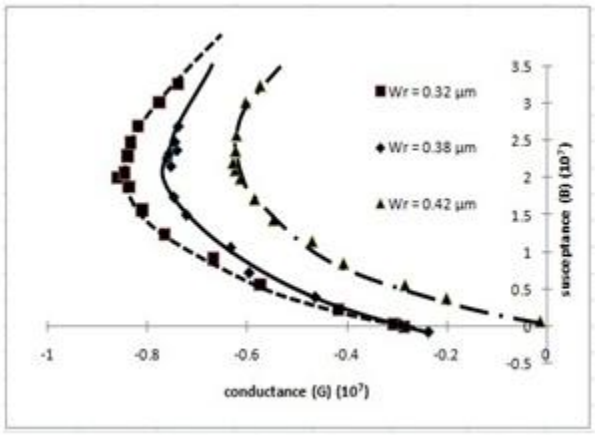

Figure 5(a). Conductance (G) vs susceptance (B) plot for different position of the charge bump w.r.t the 1st edge from the metallurgical junction.

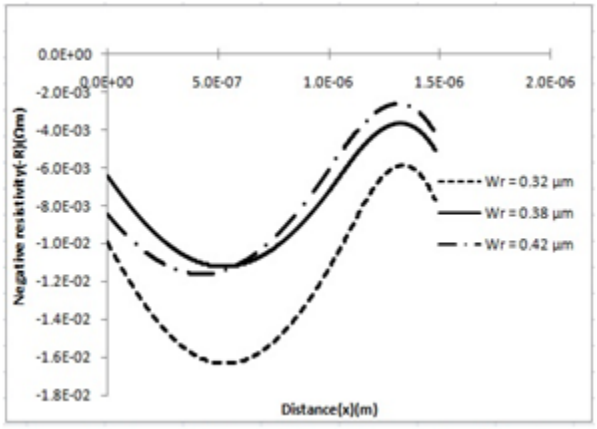

Figure 5(b). Negative resistivity profile for different position of the charge bump w.r.t. the 1st edge from the metallurgical junction.

4 CONCLUSIONS

The present study reveals the overall degradation in the performance of the GaN (Wz) based W-band IMPATT diode for shifting the charge bump position away from the junction. Changing of the width of the charge bump does not affect so much into the performance of the diode. At the same time there are some intermediate values of the height of the charge bump for which the response of the diode is quite good. This present analysis is extremely helpful in

choosing the height, width and position of the charge bump in SLHL structure for improved response of the IMPATT diode.

5 REFERENCES

[1] Okumura H, "The Present Status and Future Prospects of Wide Band Semiconductor high power devices ", 2006 Japan.J.Appl.Phys.**45** 7565

[2] Mazumder N and Roy S K, "Studies on pulsed millimeter wave low-high-low Si IMPATT diodes at high current density and dependence on structural parameters."1997 semicond.Sci. Technol.12 623

[3] J.P.Banerjee, J.F.Luy, and F.Schaffler," Comparison of theoretical and experimental 60 GHz Silicon IMPATT diode performances", Electronics Letters, vol.27, pp.1049-50, 1991.

[4] J.F.Luy, F.Scheffler, and F.Schlett,"17.6% conversation efficiency at 60 GHz with IMPATT diodes"22nd European Microwave conference (Tunbridge Wells: Microwave Exhibition and Publ.),p. 485,1992

[5] M.Wollitzer, J.Buechler, F. Schaffler, and J.F.Luy," D-band Si IMPATT diodes with 300mW CW output power at 140GHz", Electronics Letters, Vol.32, pp.122-3, 1996.

[6] M mukherjee, N Mazumder,"Effects of Charge Bump on High-Frequency Characteristics of α-SiC-based double-drift ATT Diodes at Millimeter-wave Window Frequencies"IETE Journal of Research, Vol.55, issue3, 118

[7] Electronic Archive. New Semiconductor Materials. Characteristics and properties http://www.ioffe.ru/SVA/NSM/Semicond/GaN

[8] Kunihiro K,Kasahara K, Takahashi Y and Ohno Y "Experimental evaluation of impact ionization coefficients in GaN",1999 IEEE Electron Device Lett. **20** 608

[9] B.Chakrabarti, D.Ghosh, M.Mitra '' High Frequency Performance of GaN Based IMPATT Diodes", IJEST, Vol.3 No.8, August 2011.

[10] D. Ghosh, B. Chakrabarti, Monojit Mitra "A Detailed Computer Analysis Of SiC And GaN Based IMPATT Diodes Operating at Ka, V And W Band", IJSER, vol. 3 issue 2, 2012

[11] Gummel H K and Blue J L "Small Signal Theory of Avalanche Noise in IMPATT diodes", 1967 IEEE Trans.Eletron Devices **14** 569

[12] Mukherjee M, Majumder N, Roy S K and Goswami K "GaN IMPATT Diode: a photo sensitive high power terahertz source" Semicond. Sci.Technol. **22**(2007) 1258-1267

[13] S.K.Roy, J.P.Banerjee and S.P.Pati 1985 Numerical Analysis of semiconductor devices (NASACODE IV) Dublin: Boole P 494

14] Mukherjee M, Roy S K "Wide band gap III-IV nitride based avalanche transit time diode in terahertz regime: studies on the effects on punch through on high frequency characteristics and series resistance of the device "Current Applied Physics **10**(2010) 646-651

[15] Eisele H and Haddad G I 1997 Active microwave Devices Microwave Semiconductor Device Physics ed S M Sze (New York) p 343